Relating wave frequency and pore fluid homogeneity in quasi-saturated sands

Guillaume Flood-Page[12*], *Luc* Boutonnier[1], and *Jean-Michel* Pereira[2]

[1]Egis, 38180 Seyssins, France
[2]Navier, Ecole des Ponts, Univ Gustave Eiffel, CNRS, Marne-la-Vallée, France

Abstract. P-wave velocity is regularly proposed as a proxy for water saturation when studying quasi-saturated soils. However, several authors have underlined that this velocity can only be reliably correlated to water saturation if the pore fluid is *"homogeneous"*. Using bender elements to measure compression wave velocity in quasi-saturated Fontainebleau sand, we show it is highly sensitive to both saturation and frequency. The characteristic length of pore pressure diffusion is used to explain the link between frequency, gas distribution and P-wave velocity. This criterion is shown to be fairly reliable for assessing the homogeneity of a pore fluid distribution in quasi-saturated Fontainebleau sand.

1 Introduction

Compression waves in soils are very sensitive to water saturation. For this reason, their velocity v_p has been correlated to the water saturation ratio S_r [1], Skempton's B value [1–3] or even to the liquefaction resistance of quasi-saturated soils [4]. However, it has also been shown that v_p is just as sensitive to pore fluid homogeneity as it is to water content [1,5]. As is visible in Fig. 1, while some sets of experimental data follow the theoretical trend predicted for *homogeneous* fluid distributions (shown in black for Fontainebleau sand), this is not necessarily the case.

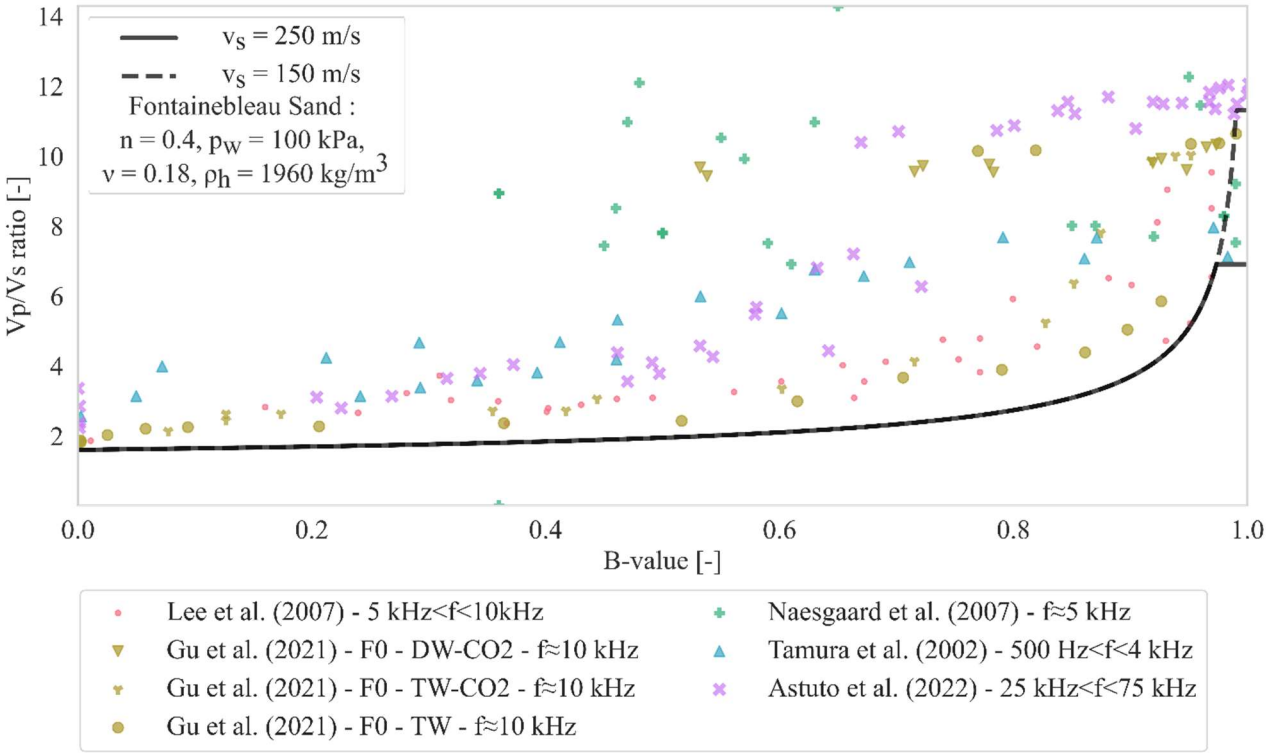

Fig. 1. Comparison in between v_p/v_s ratio and Skempton's B-value as found in geotechnical literature [1-3,5,13] and analytical values derived for Fontainebleau Sand.

* Corresponding author: gfloodpage@gmail.com

The equation relating saturation ratio S_r and P-wave velocity v_p is generally derived within the framework of linear elastic plane wave theory. Considering an undrained P-wave modulus M_u and a density ρ:

$$v_p = \sqrt{\frac{M_u}{\rho}}. \quad (1)$$

The undrained P-wave modulus can in turn be related to the undrained bulk modulus K_u. Considering the equations provided by [6] and supposing that solid grains are incompressible ($K_s \gg K_f$ and $K_s \gg K$), one can express M_u as follows:

$$M_u = K_u + \frac{4G}{3} = \frac{1 + \frac{nK}{K_f}}{\frac{n}{Kf}} + \frac{4G}{3}, \quad (2)$$

where K is the dry bulk modulus of the soil, K_f is the bulk modulus of the pore fluid, K_s is the bulk modulus of the minerals composing the solid fraction of the soil and n is the porosity. It is worth noting that this expression can also be derived from the *"Gassman equation"* [7], which is more commonly adopted by geophysicists. The dry bulk modulus is estimated via the shear wave velocity v_s, supposing a Poisson ratio ν. Skempton's B-value is computed as described in [6], considering an incompressible solid phase:

$$G = \rho {v_s}^2 \quad (3)$$

$$K = \frac{2G(1+\nu)}{3(1-\nu)} \quad (4)$$

$$B = \frac{\Delta p_f}{\Delta p} = \left(1 + \frac{nK}{K_f}\right)^{-1} \quad (5)$$

While the theoretical expressions written above are perfectly valid in the framework described by [6], their use in the context of acoustic wave propagation can be unreliable. The main issue lies with the definition of the fluid compressibility of a gas-water mixture. This can be understood within the framework of homogenisation theory.

Considering a fluid mixture composed of a water phase (index "w") and a gas phase (index "g"), the bulk modulus of the resulting mixture (index "f") will be some combination of the moduli K_g and K_w weighted by the saturation ratio S_r. The lower bound for the bulk modulus K_f of this mixture can be computed supposing the fluid pressure p_f has the time to equilibrate between stiff water-filled pores and compliant gas-filled pores. This approach results in the "*Reuss*" bound for fluid compressibility:

$$K_f = \left(\frac{S_r}{K_w} + \frac{1 - S_r}{K_g}\right)^{-1}. \quad (6)$$

This expression is sometimes also named after the works of Wood [8] and Koning [9].

Alternatively, the upper bound of the fluid bulk modulus can be estimated considering that the fluid strain ϵ_f is equal to the strain in each phase: $\epsilon_f = \epsilon_g = \epsilon_w$. This condition is only satisfied if the fluid pressure p_f does not have the time to equilibrate between more and less compressible regions. This could notably occur for soils with a very heterogeneous gas distribution as the pressure equilibration distance would be considerably greater than for homogeneous gas distributions. This approach leads to the *"Voigt"* bound for the fluid bulk modulus, sometimes named after Hill [10]:

$$K_f = S_r K_w + (1 - S_r) K_g \quad (7)$$

Looking back at Fig. 1, one can understand that, for experiments where the saturation is considered as perfectly homogeneous, the data follows the lower *Reuss* bound. For experiments where the saturation is not

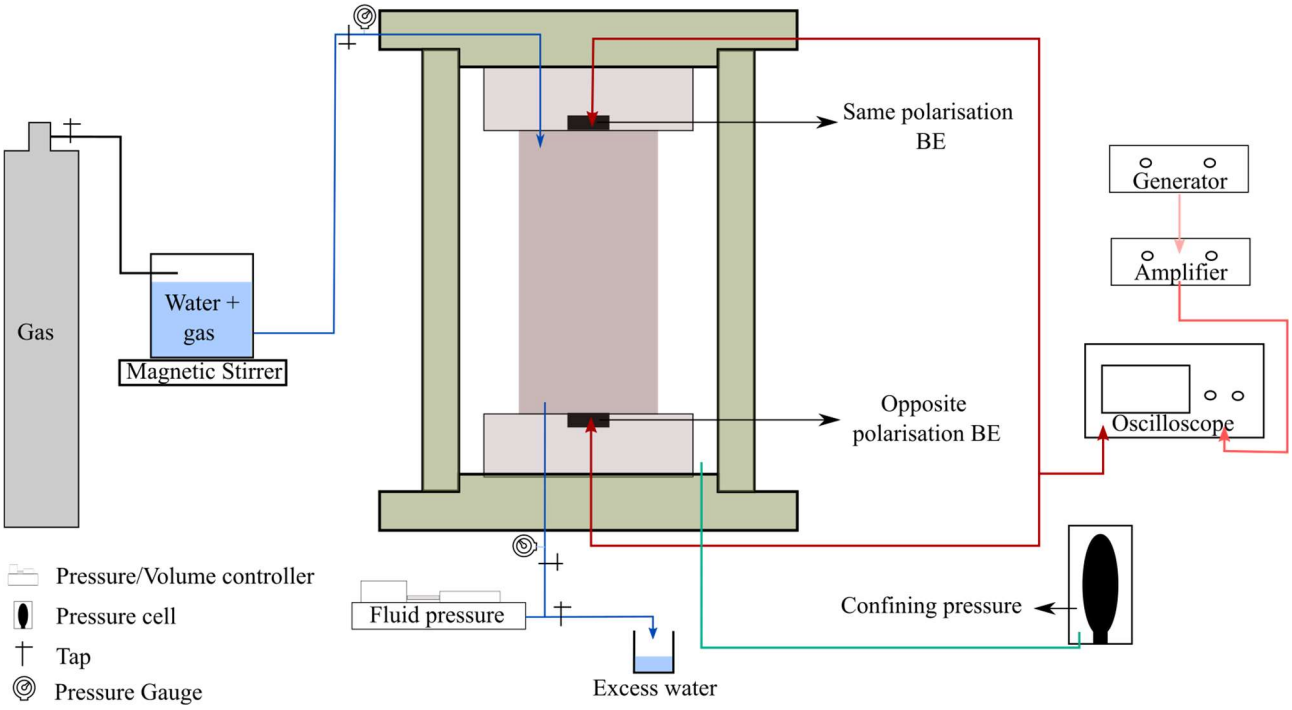

Fig. 2. : Experimental apparatus

homogeneous, the resulting v_p/v_s ratio is contained somewhere between the bounds. The main objective of this paper is to provide a quantifiable criterion to assess whether a pore fluid distribution can be described as homogeneous.

2 Laboratory data

2.1 Experimental setup

In order to propose a criterion for assessing the homogeneity at specimen scale of a gas-water mixture, a series of experiments were led on Fontainebleau sand. Compression and shear wave velocities were measured using a set of bender-extender elements (length ≈ 3.5±0.5 mm). The signal was generated with a TG1010A function generator and visualised with an Agilent Technologies InfiniiVision DSO-X-2004A digital oscilloscope.

The sand specimens are built by dry pluviation or dry tamping methods. Their diameter is 100 mm while the height varies between 100 and 200 mm. Once constructed, they are flushed with carbon dioxide for over twenty minutes, before being saturated with deaired water. Subsequently, air and water are mixed together in a closed cell at controlled pressure for at least twelve hours. A magnetic stirrer is used to accelerate the dissolution of air in the water (see Fig. 2). This *"new"* pore fluid is then injected into the specimen in order to replace the deaired pore fluid by one containing greater quantities of dissolved gas. The saturation state is changed by lowering the pore pressure to allow gas to exsolve. This desaturation method ensures that gas bubbles are mostly contained within the pores for quasi-saturated soils.

Skempton's B-value is measured by subjecting the specimen to an undrained pressure change and measuring the resulting difference in pore pressure. This process is repeated at least six times for each measurement of B. The applied pressure changes are around 20 kPa.

Table 1. List of experiments

Specimen	*e [-]*	*Preparation*	p_{sat} *[kPa]*
Id92-H200-2	0.56	Pluviation	350
Id92-H200-3	0.57	Dry tamping	350
Id92-H200-5	0.56	Pluviation	350
Id92-H100-1	0.56	Pluviation	375
Id92-H100-2	0.56	Pluviation	425
Id54-H200-1	0.69	Pluviation	410
Id54-H200-2	0.69	Pluviation	450
Id54-H200-3	0.69	Pluviation	380
Id54-H200-4	0.69	Pluviation	480
Id54-H200-6	0.69	Pluviation	400

Table 1 contains a list of all specimens prepared in the context of this study on quasi-saturated Fontainebleau sand. The name of each specimen indicates its density index I_d and height H. The number at the end distinguishes different specimens with the same density. The saturation pressure p_{sat} is an estimation of the water pressure at which the saturation ratio begins to decrease during each experiment.

2.2 Properties of Fontainebleau sand

In order to interpret these experiments, the following data was considered for the median grain size D_{50}, uniformity coefficient C_u, minimum and maximum void ratios $e_{\min}$ and $e_{\max}$, and grain density ρ_s for Fontainebleau sand. The data is taken from [11].

Table 2. Properties of Fontainebleau sand

D_{50} *[mm]*	C_u	e_{min}	e_{max}	ρ_s *[t/m³]*
0.223	1.48	0.545	0.866	2.65

Small-strain moduli were determined on dry Fontainebleau sand specimens. The detail of this process is explained in [12]. Fitting the experimental data provides the following estimations of the small-strain shear modulus G_0 and a Poisson ratio ν of 0.18 (with p' the effective stress and P_{ref} atmospheric pressure):

$$G_0 = 99.98\left(\frac{p'}{P_{ref}}\right)^{0.52}. \quad (8)$$

In order to interpret B measurements, the small-strain moduli mentioned previously did not seem relevant as the strain range is completely different. Therefore, drained isotropic consolidation tests were carried out on saturated Fontainebleau sand. The volume changes were measured using the pressure-volume controller (see Fig. 2). Using this method, separate fitting curves were obtained for different stress states. As all experiments were performed on overconsolidated soils, only the overconsolidated fit is provided here. A slight discrepancy was noted between the overconsolidated bulk moduli calculated during unloading and reloading phases. As a first approach, this difference was not taken into account as the resulting error is small. The equation given below corresponds to the drained bulk modulus of overconsolidated Fontainebleau sand during a reloading phase:

$$K = 19.99\frac{(2.98-e)}{1+e}\left(\frac{p'}{P_{ref}}\right)^{0.46}. \quad (9)$$

3 Experimental analysis

3.1 Methodology

As shown by [13], detecting P-waves in gassy soils using bender elements is generally quite complex as signals can contain different components propagating at varying velocities. This renders the frequency-velocity interpretation of these signals fairly imprecise.

To limit this error, measurements are made at over twenty different input frequencies ranging in between 2 and 200 kHz. After eliminating poor quality signals, the arrival time is determined using the SLA time domain method described in [12]. This automated interpretation method is based on a statistical tool named *"Akaike Information Criterion"* and gives similar results to the *"First Arrival"* method. The frequency of the actual signal is then estimated by Fourier transform over a 1 millisecond fraction of signal after the arrival. This limits the influence of any other existing wave components on the calculated frequency.

Finally, data points are grouped by frequency range. The size of the frequency ranges is chosen in a way to ensure there are always a few signals per range. It also gives an indication of the precision of the frequency estimation. The considered P-wave velocity for each frequency range is its median velocity. The shear velocity is also measured at different frequencies for each stage of the experiment. As v_s is not frequency dependant, the adopted value is the median of all calculated shear wave velocities.

3.2 Experimental observations

Figures 3 and 4 show the evolution of the v_p/v_s ratio as a function of B for Fontainebleau sands with density indexes I_d respectively equal to 0.54 and 0.92.

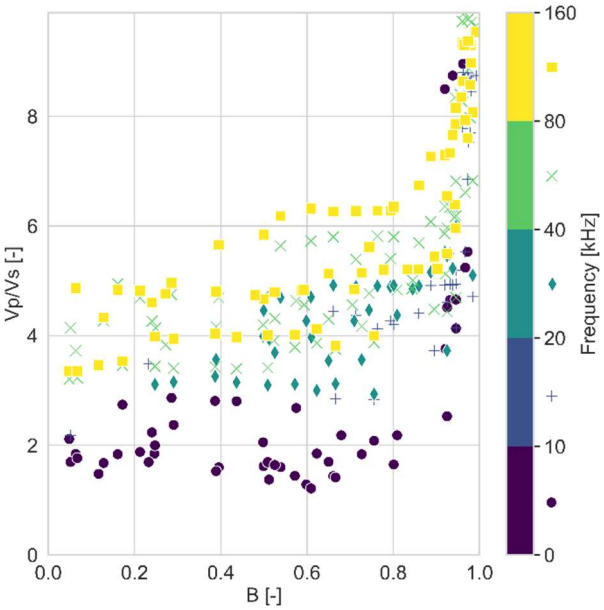

Fig. 3. v_p/v_s ratio as a function of B value and frequency for Fontainebleau sand with $I_d \approx 0.54$

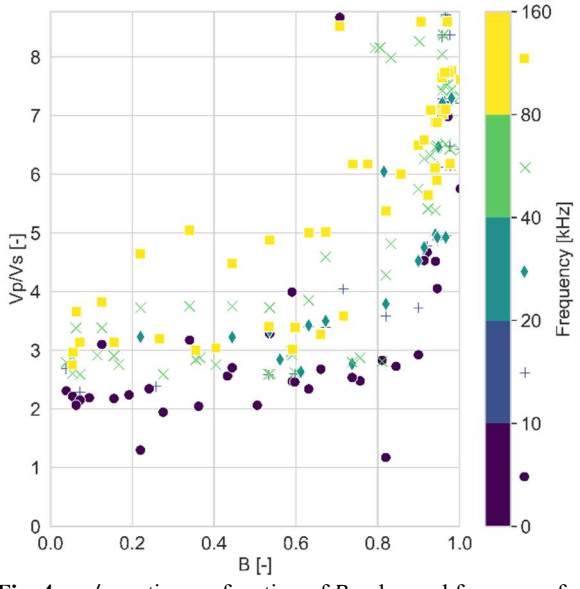

Fig. 4. v_p/v_s ratio as a function of B value and frequency for Fontainebleau sand with $I_d \approx 0.92$

We observe a clear dispersion of the P-wave velocity with frequency. As a rule, the lowest frequencies behave in a manner fairly consistent with velocities computed using the *Reuss* bound for equivalent fluid compressibility (black lines plotted in Fig. 1). However, as frequency increases, the experimental data progressively departs from this prediction.

One can also notice that this frequency dispersion is only truly observable for *"gassy"* specimens (B<0.95). While there is a slight spread for *"saturated"* data points, this is mostly due to measurement error and temperature variations in the laboratory (in between 15 and 23°C).

Therefore, we can conclude that the dispersion observed in this study and in Fig. 1, is not only a matter of gas distribution as proposed by [1,5], but also a function of frequency.

4 Interpretation

4.1 A criterion for gas homogeneity

The topic of P-wave dispersion in the presence of partly saturated porous media has previously been explored in the field of petroleum geophysics. Norris [14] uses a characteristic pore pressure diffusion length L_d to assess the homogeneity of gas/water mixtures in Berea sandstone.

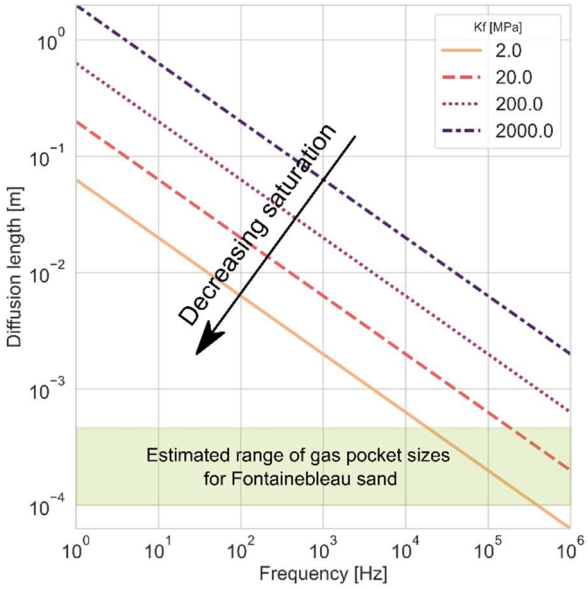

Fig. 5. Estimation of the pressure diffusion length for Fontainebleau sand (I_d = 0.54)

L_d describes the length scale over which pore pressure will dissipate under the effect of a passing compression wave. It can be computed considering the fluid bulk modulus K_f, the intrinsic permeability κ, the fluid dynamic viscosity η, the porosity n and the angular frequency ω of the wave:

$$L_d = \sqrt{\frac{\kappa K_f}{\eta n \omega}}. \qquad (10)$$

For Fontainebleau sand, this diffusion length is plotted in Fig. 5. Despite being given for a density index of 0.54, the

graph also holds for denser sands as the impact of porosity is negligible when compared to the variations in fluid bulk modulus. We consider a hydraulic conductivity of approximately 5.10^{-5} m/s (taken from [15]), and fluid bulk moduli varying from 2.10^{3} (saturated) to 2 MPa (low saturation: B<0.1).

To ensure that the *Reuss* average is valid, local excess pore pressure generated at the peak of a compression wave must have enough time to dissipate before the next peak arrives. Therefore, if the characteristic diffusion length L_d is much greater than the scale of saturation heterogeneities (deduced here from the pore size distribution), the *Reuss* bound for K_f should be valid. Looking at Fig. 5, this condition is potentially met for the lowest tested frequencies (under 10 kHz). For any higher frequencies, there does not seem to be an order of magnitude between the patch sizes and the diffusion length. For this reason, we cannot assume that pore pressures are at equilibrium

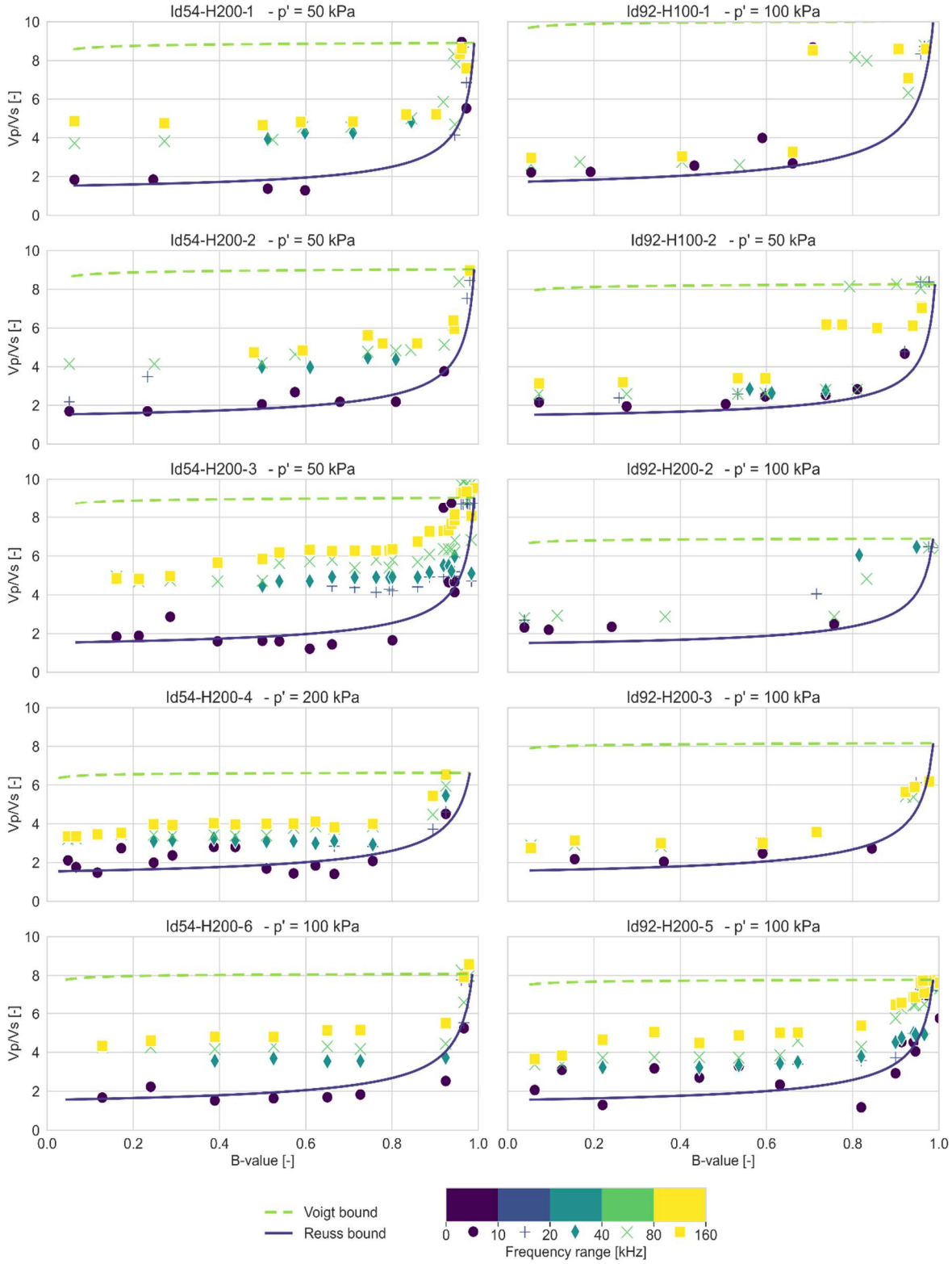

Fig 6. Comparing Reuss and Voigt theoretical bounds with experimental values of v_p/v_s ratio and B value

for frequencies above 10 kHz. Conversely, for all frequencies tested here, the typical scale of saturation heterogeneities is not an order of magnitude greater than the diffusion length. For this reason, the strain field is not expected to be homogeneous for any frequency ($\epsilon_g \neq \epsilon_w$).

All in all, this diffusion length helps explain why the *Reuss* bound is potentially valid only for the lowest tested frequencies, while the *Voigt* bound always predicts P-wave velocities higher than those measured in this experiment. . Returning to Fig. 1, experimental data from [1] (where CO_2 flushing is used) and [2] seems to follow similar trends to what was observed here for low frequency signals, whereas data from [1] (no CO_2 flushing) and [3,5,13] does not. This is understandable as the first set of experiments use desaturation methods that would ensure a fairly homogeneous gas distribution combined with relatively low frequencies. By contrast, the other sets of data either use higher frequencies or desaturation methods that create more heterogeneous gas distributions.

4.2 Assessing the validity of the Reuss bound for low frequency waves

Fig 6 plots the evolution of the v_p/v_s ratio separately for each experiment. This allows for an accurate plot of the theoretical values predicted by the *Reuss* and *Voigt* bounds. Bearing in mind the considerable error in the estimation of both the frequency and P-wave velocity, our data seems to indicate that the *Reuss* average is fairly accurate for frequencies below 10 kHz. This is consistent with the predictions of the diffusion length L_d shown in Fig. 5, indicating that local excess pore pressure does have time to dissipate for these frequencies. Therefore, the characteristic diffusion length L_d seems to be a reliable criterion for assessing the validity of the *Reuss* bound.

Concerning frequencies higher than 10 kHz, the experimental data shows that neither the *Reuss* nor the *Voigt* bound is accurate. Again this is compatible with the proposed criterion as the diffusion length is of the same order of magnitude as the gas pockets. Unfortunately, we were unable to generate input signals with frequencies higher than 200 kHz and therefore cannot verify that the experimental data does tend towards the *Voigt* bound for very high frequencies.

5 Conclusion

Through an experimental study of the impact of saturation and frequency on P and S wave velocities, we have shown that, for Fontainebleau sand, the pore pressure diffusion length proposed by [14] seems to be an accurate criterion for assessing the homogeneity of a gas-water mixture.

So long as another dispersion mechanism is not encountered, this criterion should therefore be reliable when assessing the validity of the *Reuss* approximation. In the context of in-situ geophysics, frequencies rarely exceed several hundred Hertz. Consequently, for Fontainebleau sand, we can infer that the *Reuss* bound could reliably be used to estimate the saturation ratio from P and S wave velocities if the average scale of saturation heterogeneities is smaller than a centimetre. However, the same is not necessarily true for other types of soils. For instance, in the case of clays, both permeability and gas pocket sizes are likely to be much smaller. Therefore, further analysis is required to ensure the validity of the *Reuss* approximation for interpreting in-situ geophysical data in soils other than sands.

We would like to mention the immense help provided by the technical team at Navier. This paper would not exist without them. We are also thankful for the regular advice and insights of Pierre Delage, Alain Pecker and Santiago Solazzi.

References

1. X. Gu, K. Zuo, A. Tessari, and G. Gao, Soil Dynamics and Earthquake Engineering **145**, 106742 (2021)
2. S.-H. Lee, Y.-W. Choo, J.-U. Youn, and D.-S. Kim, Journal of the Korean Geotechnical Society **23**, 71 (2007)
3. S. Tamura, K. Tokimatsu, A. Abe, and S. Masayoshi, **42**, 121 (2002)
4. L. Mele, J. T. Tian, S. Lirer, A. Flora, and J. Koseki, Géotechnique **69**, 541 (2019)
5. E. Naesgaard, P. M. Byrne, and D. Wijewickreme, Int. J. Geomech. **7**, 437 (2007)
6. A. W. Bishop, 8 (1973)
7. F. Gassmann, 22 (1951)
8. A. B. Wood, *A Textbook of Sound* (1941)
9. H. L. Koning, Proc. of the European Conf. on SMFE **1**, 33 (1963)
10. R. Hill, Journal of the Mechanics and Physics of Solids **11**, 357 (1963)
11. I. Andria-Ntoanina, Caractérisation Dynamique de Sables de Référence En Laboratoire - Application à La Réponse Sismique de Massifs Sableux En Centrifugeuse, Université Paris-Est, 2011
12. G. Flood-Page, J.-M. Pereira and L. Boutonnier, (To be published)
13. G. Astuto, F. Molina-Gómez, E. Bilotta, A. Viana da Fonseca, and A. Flora, Acta Geotech. (2022)
14. A. N. Norris, The Journal of the Acoustical Society of America **94**, 359 (1993)
15. S. Feia, J. Sulem, J. Canou, S. Ghabezloo, and X. Clain, Acta Geotech. **11**, 1 (2016)